

IRON LOSS ANALYSIS METHOD USING IRON LOSS CURVES ACCORDING TO FREQUENCY

Hyuk Nam, Jeong-Jong Lee, Ki-chang Chang, and Jung-Pyo Hong, Senior Member, *IEEE*

Dept. of Electrical Eng., Changwon Nat'l Univ., Changwon, Gyeongnam, 641-773, Korea
haeggee@korea.com, wave95@korea.com, namhyuk3@empal, jphong@sarim.changwon.ac.kr

Abstract—This paper deals with an iron loss analysis method in the single-phase line-start permanent magnet synchronous motor. The iron loss is affected by the time rate of the change of magnetic flux density in the motor cores. The distribution and changes in magnetic flux densities of the motor are computed by using 2-dimensional finite element method. Discrete Fourier Transform is used to analyze the magnetic flux density waveforms in each element of the analysis model. Iron losses in each element are evaluated using iron loss curves according to frequencies and harmonic analysis results. The total iron loss can be obtained by the summation of the iron losses in all elements.

Introduction

Capacitor-run single-phase induction motors (SPIMs) are widely used in household applications because of direct operation fed capability from the commercial single-phase voltage source without any control devices. However, the resistances and the induced currents in the conductor bars induce the slip power loss, which causes low overall efficiency. On the other hand, single-phase line-start permanent magnet synchronous (LSPM) motors are essentially induction motors with permanent magnet materials inserted in the rotor, i.e., these motors have rotor cages for induction starting and permanent magnets, providing synchronous torque. Since these motors operate as a synchronous machine, the induced currents in the rotor are much smaller than that of induction machines. Therefore, the slip power loss in the rotor can be significantly reduced and additionally it is possible to achieve unity-power-factor performance, thereby reducing the stator currents and the corresponding losses [1].

In spite of the excellent performance of LSPM motors, their optimal utilization requires attention to many aspects related to the machine design and performance. In this respect, the calculation of iron losses, which can be a major part of total losses, is particularly challenging since it requires an accurate prediction of the magnetic flux density distribution in both spatial and temporal coordinates and the corresponding iron loss [2], [3].

In traditional ac machine theory the iron loss is viewed as being caused mainly by the fundamental frequency. Normally, under alternating flux conditions, the iron loss P_c in W/kg is separated into a hysteresis loss component P_h , and an eddy current component P_e , both in W/kg , as shown in equation (1).

$$P_c = P_h + P_e = k_h f B_m^\alpha + k_e f^2 B_m^2 \quad (1)$$

where f and B_m are the frequency and the peak value of the magnetic flux density, respectively. K_e , k_h and α are constants provided by the manufacturer. This conventional method assumes sinusoidal variation of the magnetic flux density waveforms. However, in most cases, it is not sufficiently accurate because the magnetic flux density waveforms are non-sinusoidal [3], [4]. In order to take into account the harmonic effects of the magnetic flux density waveforms on the iron loss, accurate prediction of the magnetic flux densities throughout the stator and the rotor cores are strongly required [5].

This paper deals with the iron loss analysis method considering harmonics of the magnetic flux density waveforms using iron loss curves according to frequency in the LSPM motor. The temporal and the spatial variations of the magnetic flux density waveforms are derived by performing 2-dimensional finite element method (2-D FEM). Discrete Fourier Transform (DFT) is used for the frequency analysis of the time-varying magnetic flux density waveforms at each element of the finite element (FE) analysis model. The iron losses in each element are calculated from iron loss curves that are expressed as iron loss curves according to frequencies and magnetic flux densities. Finally, the total iron loss is obtained by the summation of the iron losses in all the elements and the result of the iron loss calculation is used for the accurate efficiency assumption of the LSPM at the steady state.

Procedure for Iron Loss Analysis

The flow chart of the method for the iron loss analysis in the paper is shown in Fig. 1 [6].

For the finite element (FE) analysis of the first step in this figure, the governing equation from Maxwell's electromagnetic equation is as follows [5], [6].

$$\nabla \times \nu (\nabla \times \vec{A}) = \vec{J}_0 + \vec{J}_e + \vec{J}_M \quad (2)$$

where ν is the magnetic reluctivity, \vec{A} is the magnetic vector potential, \vec{J}_0 is the current density of the coil, \vec{J}_e is the eddy current density, and \vec{J}_M is the equivalent magnetization current density. In this equation, the current density of the coil can be calculated from the voltage equations of the main and the auxiliary windings [6]. The skew effect is ignored in this FE analysis.

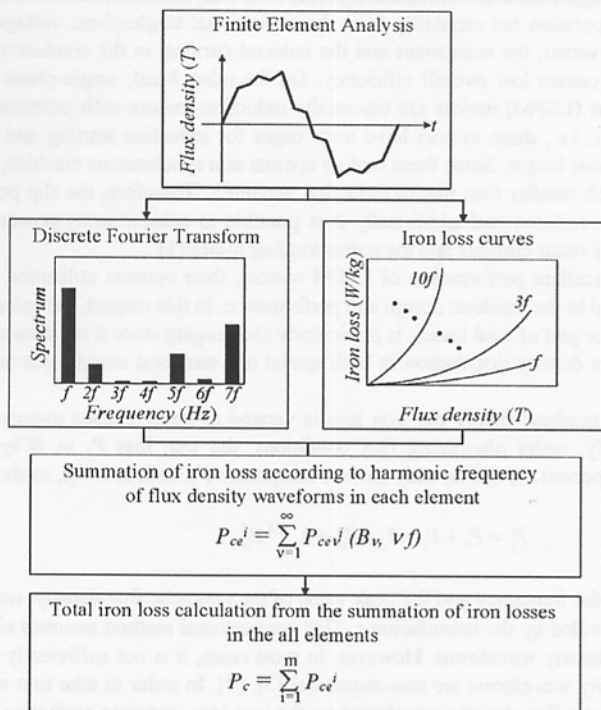


Fig. 1 Flow chart for iron loss calculation

DFT for harmonic analysis of the magnetic flux density waveforms are computed by FEM at the first step can be expressed as equation (3).

$$B_{pk}(k) = \sum_{n=0}^{N-1} B_p(n) e^{j \frac{2\pi nk}{N}} \quad (3)$$

where k is the harmonic order, N is the number of the discrete data, $B_{pk}(k)$ is the peak value of the magnetic flux density of the k -th harmonic, and $B_p(n)$ is the magnitude of the point n ($n=0, 1, 2, \dots, N-1$).

At final step, the iron losses P_{ce}^i in each element are calculated from iron loss curves that are expressed as iron loss curves according to frequencies and magnetic flux densities and then, the total iron loss P_c is obtained by the summation of the iron losses in all the elements

Experimental Results at the Rated Condition

Fig. 2 shows the cross-section of the analysis model. The motor has two windings, a main winding connected directly to the 115V, 60Hz supply, and an auxiliary winding connected to the supply via capacitor. Rotor has the permanent magnets and the conductor bars are inserted in the rotor as shown in Fig. 2.

Fig. 3 and Table. 1 show the test apparatus and the experimental results at the rated condition. Total loss in the motor is about 21.00W including winding copper losses of 8.67W. Therefore, Iron loss, stray load loss, and conductor loss in the rotor are about 12.33W, that is, these losses occupy about 58.7% in the total losses.

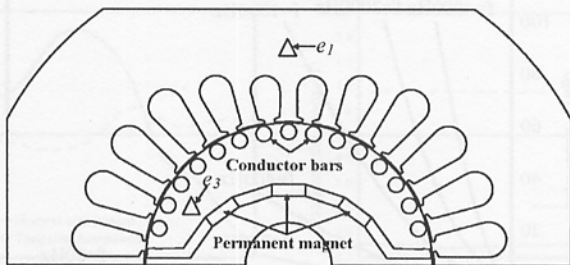


Fig. 2 Cross-section of the analysis model

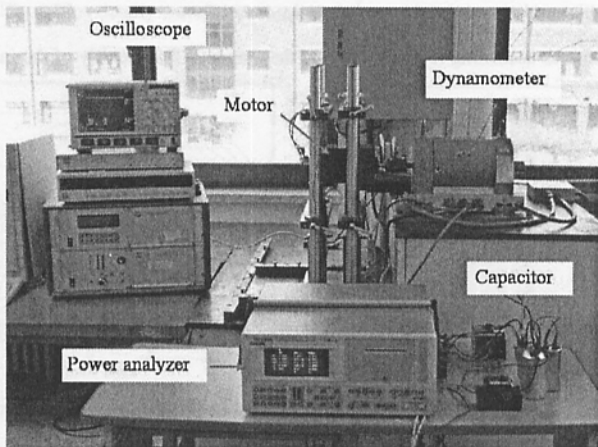


Fig. 3 Test apparatus

Table. 1 Experimental results at the rated condition

Input power (W)	Output power (W)	Winding copper loss (W)	Efficiency (%)
181.00	160.00	8.67	88.39

Analysis Results

Fig. 4 presents the iron loss curves according to frequencies and the magnetic flux density of the magnetic material.

As the rated currents are applied at the steady state, the distribution of the equipotential with angular position is shown in Fig. 5.

Fig. 6, and Fig. 7 show the component magnetic flux density waveforms at different locations in the stator and the rotor, that is, e_1 , and e_2 in Fig. 2, and the DFT results of the waveforms, respectively. In Fig. 6, while the distribution of the magnetic field of e_1 that represents a position in the stator yoke has equal frequency to the rotating magnetic field, and the tangential component of the magnetic flux density leads the normal component, that of e_2 that shows a position in the rotor yoke is expressed as dc components because the rotation of the rotor synchronizes with that of the rotating magnetic field.

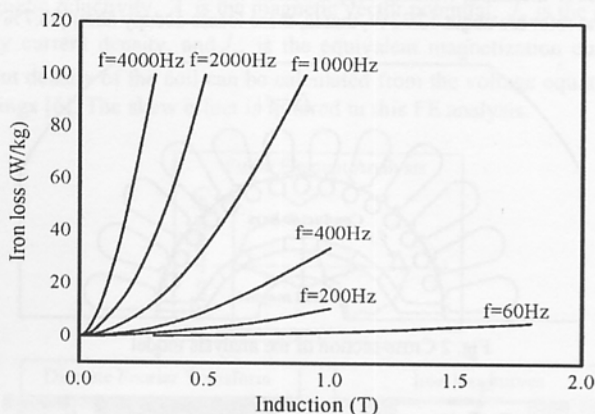


Fig. 4 Iron loss curves according to frequency and the magnetic flux density of the magnetic material

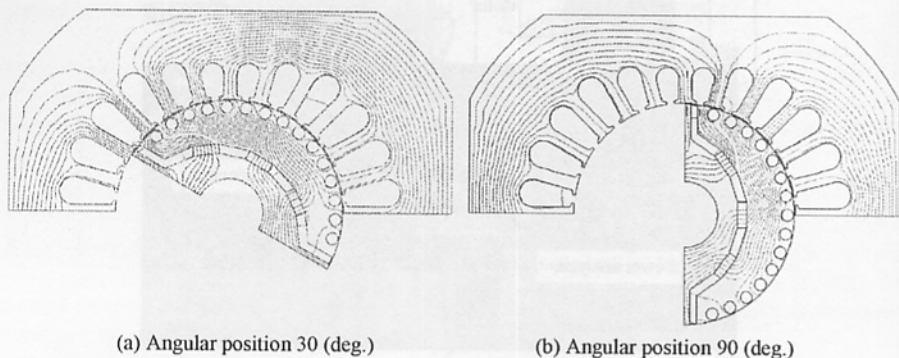


Fig. 5 Equipotential lines at the steady state

Fig. 7, where the fundamental frequency is 60 Hz, shows the harmonic analysis results of the magnetic flux density waveforms in Fig. 6(a).

Fig. 8 presents the iron loss components from the fundamental component to the 12th harmonic component according to the harmonic order.

From the results, the total iron losses to the 12th harmonic component are 12.10 W, and the losses except for the fundamental component is about 9.41 W that occupies about 77.77 % in the total iron loss. Therefore, it is very important to analyze the iron loss considering the harmonic components in the magnetic flux density waveforms.

Conclusion

This paper deals with the iron loss analysis using iron loss curves according to frequencies and the harmonic analysis results of the time-varying magnetic flux density waveforms calculated by 2-D FEM.

The total iron loss to the 12th harmonic component is 12.10W, and the loss except for the fundamental component is about 9.41W that occupy about 77.77% in the total iron loss. The analysis result shows that the harmonic components of the magnetic flux waveforms should be considered to evaluate the accurate iron loss. Moreover, when the iron loss is compared with the loss of 12.33W, except for the winding copper loss of 8.67W by the experiment, the loss of 0.23W remains. It is supposed that the loss contains the iron loss by the harmonic components and the losses such as the stray load loss and the conductor bar loss by the unbalanced magnetic field is not considered in the analysis.

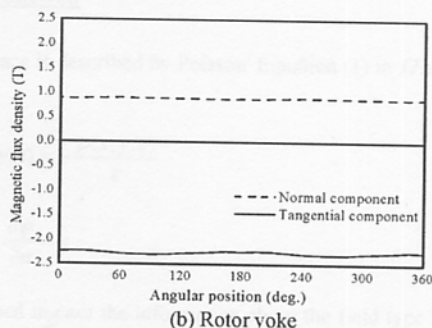
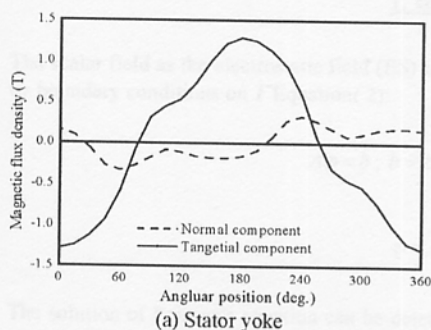


Fig. 6 Flux density waveforms at selected sites with motor angular position

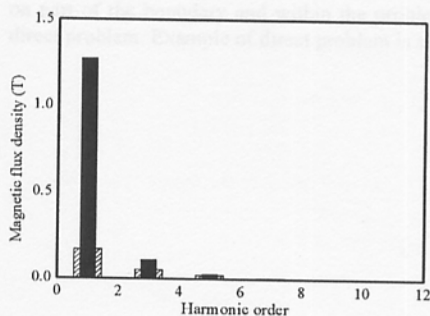


Fig. 7 Harmonic analysis results at the stator yoke

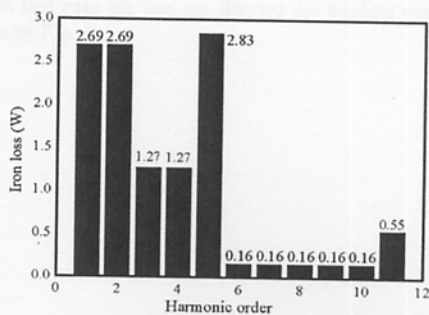
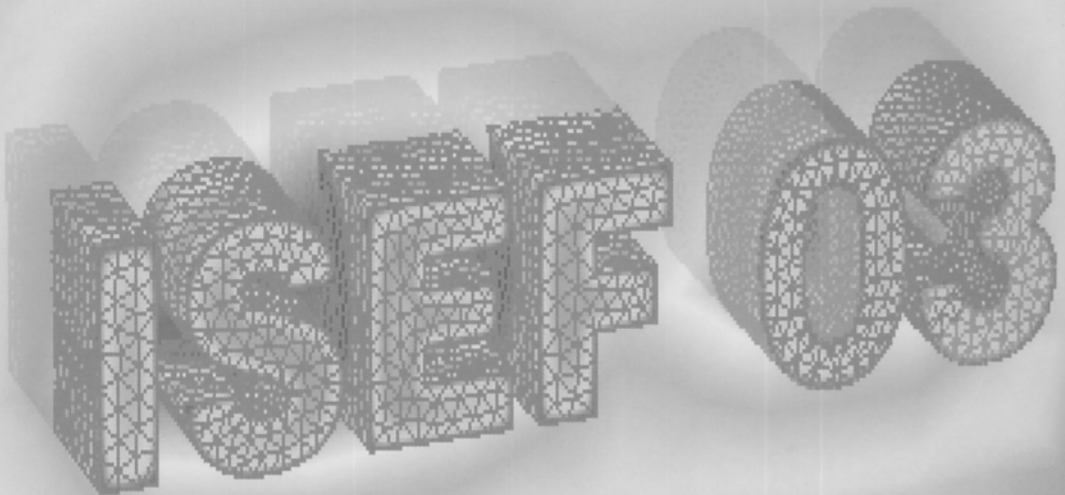


Fig. 8 Iron loss with the harmonics



XI INTERNATIONAL SYMPOSIUM
ON **ELECTROMAGNETIC FIELDS**
IN ELECTRICAL ENGINEERING
ISEF 2003



SEPTEMBER 18-20, 2003

MARIBOR, SLOVENIA

The Symposium is organised by:

- Research group Applied Electromagnetics, Faculty of Electrical Engineering and Computer Science, Maribor, Slovenia
- University of Maribor, Slovenia
- Institute of Mechatronics and Information Systems, Technical University of Lodz, Poland
- Department of Fundamental Research, Electrotechnical Institute, Warsaw, Poland

VOLUME 1

15. A Method for Reduction of Cogging Torque in PM Machines Using Stepped Magnets M. Łukaniszyn, R. Wróbel, M. Jagieła	511
16. Iron Loss Analysis Method Using Iron Loss Curves According to Frequency H. Nam, J.J. Lee, K.C. Chang, J.P. Hong	517
17. Inverse Problem - Determining Unknown Distribution of Charge Density Using the Dual Reciprocity Method D. Ogrizek, M. Trlep	523
18. Application of Boundary – Approximated Method for the Analysis of Electromagnetic Field Near by Conducting Corner S. Pawłowski	529
19. An Analysis of Transformation of Commutation Events to a Stator Voltage Waveform J. Rejec, B. Benedičič, F. Pavlovčič, J. Nastran	535
20. Comparison of the General Load Line Method with the Finite Element Method R. I. Román, B. A. Konrad, J. F. Brudny	541
21. The Optimal Design of Passive Shimming Elements for High Homogeneous Permanent Magnets Utilizing Sensitivity Analysis Y. Yao, C. S. Koh, G. Ni, S. Yang, D. Xie	547
22. 3D Shape Optimization of Eddy Current Problems Using Design Sensitivity Analysis Y. Yao, J. S. Ryu, C. S. Koh, D. Xie, P. S. Shin	553
23. Development of Mathematical Model and Computation of Electromagnetic Drum-Type Separator by Boundary Element Method M.V. Zagirnyak, O.S. Akimov	559
24. Improvement of a Quadrosection Method for the Complicated Equivalent Circuit Computation M. V. Zagirnyak, V. M. Usatyuk, O.S. Akimov	565
25. Calculation and Modelling of Earth Grounding A. Zarrouki, F. Ghodbane, M. Javoronkov	571

ORAL SESSION:

ELECTROMAGNETIC ENGINEERING 4 (EE-4, Micro and Special Devices) [14.45-16.45]

Chairman: Prof. A. Krawczyk

1. Electromechanical Study of Micromachined Electrostatic Parallel-Plate Actuators J. De Coster, F. Henrotte, K. Hameyer, R. Puers	577
2. Determination of a Dynamic Radial Active Magnetic Bearing Model Using the Finite Element Method B. Polajžer, G. Štumberger, D. Dolinar, K. Hameyer	581